DOI: https://doi.org/10.54966/jreen.v6i2.968 Rev. Energ. Ren. Vol.6 (2003)131-141

Spatial Adaptation Procedure on Unstructured Meshes for Steady and Unsteady Flows around Bluff-Bodies

Abbes Azzi

Laboratoire de Mécanique Appliquée, Faculté de Mécanique, Université des Sciences et de la Technologie d'Oran, B.P. 1505 El'mnaouar, Oran, Algérie

Abstract – *Two-dimensional, compressible Euler and Navier-Stokes equations are solved numerically by finite volume method to predict steady and unsteady flows around bluff-bodies. An unstructured grid generator code is linked in an automatic way to the flow solver within a spatial adaptation procedure. The aim is to predict complex compressible flows such as shock waves and separated boundary layers with accurate and efficient calculations. Computational results for many test cases are compared successfully with published data.*

Résumé – *Les équations d'Euler et les équations de Navier-Stokes pour un écoulement bi-dimensionnel, compressible, stationnaire et non stationnaire sont résolues en utilisant une méthode numérique aux volumes finis. En vue d'optimiser la procédure de calcul, le générateur de maillage non structuré et le code de calcul sont liés dynamiquement via une procédure d'adaptation spatiale de la grille de calcul. Le but étant de prédire économiquement et efficacement des phénomènes complexes tels que les ondes de chocs et le détachement de la couche limite. Les résultats numériques de plusieurs cas tests sont comparés avec succès aux données publiées dans la littérature.*

Keywords: Euler equations – Navier-Stokes equations – Finite volume method – Unstructured grids – NACA0012.

1. INTRODUCTION

In recent years, great developments in algorithms for Euler and Navier-Stokes equations on unstructured grids have occurred. The popularity of this new trend in grid generation is motivated principally by two main advantages. The first one is the simplicity of grid generation for complex geometries compared to that of block structured grids, particularly for complicated three-dimensional cases. The second advantage is the local concentration of the grid points in locations of interest such as that in the near-field region of any object. This operation can be done through a dynamic way known as adaptive mesh refinement. This technique is achieved by adding points in regions where solution gradients are relatively large and removing points where they are not needed. The advantage of such procedure is to produce higher spatial accuracy at minimal computational cost. Similar techniques are the temporal adaptation which is used to improve explicit time-marching schemes for unsteady aerodynamics applications. A comprehensive discussion related to these techniques is presented by Bartina [1].

The most popular unstructured grids are composed of triangles or tetrahedra, depending on the nature of the computational domain, which can be respectively, two and three dimensional. The robustness of the unstructured-grid solver is principally due to upwind schemes used in finite-volume discretisation of the governing equations. Recently, various upwind schemes are available either in cell-centered or cell-vertex formulations. Many recent references [2-4] provide a review and state of the art of unstructured grids and finite-volume solvers.

In order to generate accurate, reasonable and economical grids, upwind high order schemes must be implemented rather than classical first-order ones. The higher-order schemes improve the resolution and reduce discontinuities in critical regions. Unfortunately, these schemes are often associated with non-physical oscillations. These oscillations can be suppressed using the modern upwind schemes that use limiters as the MUSCL approach [5]. The tendency of adversely affecting the convergence of the solution to steady state associated with such techniques is successfully avoided by using the differentiable limiters [6]. A key comparative study of multi-dimensional limiters schemes is reported in [7]. Most compressible solvers use collocated scheme because non staggered grids do not lead to the known pressure oscillations as with incompressible flow. However, in a recent study Wenneker et al. [8] proposed a staggered scheme which has the advantage to be applied simultaneously to compressible and incompressible flows.

2. GOVERNING EQUATIONS AND NUMERICAL METHOD

The governing equations for two-dimensional viscous compressible flow in Cartesian coordinates can be expressed in nondimensional form as [9]:

$$\frac{\partial U}{\partial t}+\frac{\partial (F-F_V)}{\partial x}+\frac{\partial (G-G_V)}{\partial y}=0, \tag{1}$$

where

$$U=\begin{pmatrix}\rho\\ \rho u\\ \rho v\\ \rho E\end{pmatrix},\qquad F=\begin{pmatrix}\rho u\\ \rho u^2+p\\ \rho uv\\ \rho uH\end{pmatrix},\qquad G=\begin{pmatrix}\rho v\\ \rho uv\\ \rho v^2+p\\ \rho vH\end{pmatrix} \tag{2}$$

$$F_V=\frac{1}{Re}\begin{pmatrix}0\\ \tau_{xx}\\ \tau_{xy}\\ u\tau_{xx}+v\tau_{xy}-q_x\end{pmatrix},\qquad G_V=\frac{1}{Re}\begin{pmatrix}0\\ \tau_{xy}\\ \tau_{yy}\\ u\tau_{xy}+v\tau_{yy}-q_y\end{pmatrix} \tag{3}$$

with

$$\tau_{xx}=2\mu\frac{\partial u}{\partial x}-\frac{2}{3}\mu\left(\frac{\partial u}{\partial x}+\frac{\partial v}{\partial y}\right),\qquad \tau_{yy}=2\mu\frac{\partial v}{\partial y}-\frac{2}{3}\mu\left(\frac{\partial u}{\partial x}+\frac{\partial v}{\partial y}\right),$$

$$\tau_{xy}=\mu\left(\frac{\partial u}{\partial y}+\frac{\partial v}{\partial x}\right) \tag{4}$$

and

$$q_x=-\frac{\mu}{(\gamma-1)M_\infty^2\,Pr}\frac{\partial T}{\partial x}\quad\text{and}\quad q_y=-\frac{\mu}{(\gamma-1)M_\infty^2\,Pr}\frac{\partial T}{\partial y} \tag{5}$$

Then, the integral form of the equations can be written as:

$$\iint_A\frac{\partial U}{\partial t}dx\,dy+\iint_A\left[\frac{\partial (F-F_V)}{\partial x}+\frac{\partial (G-G_V)}{\partial y}\right]dx\,dy=0, \tag{6}$$

where A is the area of the computational cell.

The finite-volume approach is based on the physical concept of using macroscopic control volumes to numerically solve the governing equations. In this study we use the so called cell-vertex technique, where the flow variables are stored at the nodes and the control volume at a given node is typically taken to that of the neighboring cells which have a vertex at that node. The 2D Navier-Stokes solver used for the present flow computation is the NSC2KE code of Mohammadi [10]. The governing equations are solved by a finite volume upwind technique using a Roe Riemann [11] solver for the convective part of the equations. The viscous terms are treated using a standard Galerkin technique and the second order accuracy of the upwind scheme is realized by a MUSCL limiter. The algorithm used is explicit in time and the steady solution is reached by an iterative scheme. The fourth order Runge-Kutta scheme allows accurate computation of time dependent flows.

3. INVISCID COMPRESSIBLE FLOW PAST A TYPICAL AIRFOIL

The test case used to validate the present solver, corresponds to a transonic flow with free-stream Mach number $(M_\infty = 0.80)$ and angle of attack $(\alpha = 1.25°)$ past a NACA 0012 airfoil. This case is characterized by the presence of a strong shock wave on the upper surface and a weak one on the lower surface. So it is necessary to compute the flow with limiters to avoid numerical oscillations that may occur in their neighborhood. This flow was considered as a test case by the AGARD reference [12] and numerous researchers among them [13] and [7]. In most previous computations, the upper surface shock wave is more or less clearly captured while the lower one is generally not captured.

The outer boundary of the computational domain is a circle located 12 chord lengths away from the airfoil. The adaptation process starts with relatively coarse mesh and after some iteration, the regions of relatively large dicretisation errors are detected so that the grid can be locally refined in order to improve the spatial accuracy. At the same time, cells are removed where they are not needed in order to reduce the computational costs. These steps are looped until an optimal grid is reached. A mesh swapping procedure can be also applied to obtain triangles as equilateral as possible. Using the MESH2D [14] code, the calculations start with a very coarse mesh and then adapted every 500 iterations. The variables chosen to define the interpolation parameter are the conservative variables and the total pressure. The last grid, composed by 17770 points, 34464 elements and 1044 points on the airfoil surface is showed on figure 1 and retained for the numerical calculations. One can see clearly the grid refinement obtained near the airfoil wall and in the vicinity of the two shock waves.

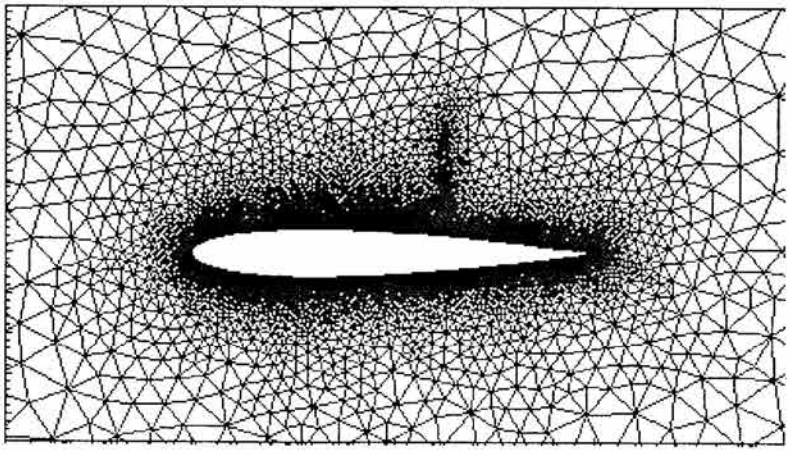

Fig. 1: Close-up of adaptive meshes for NACA 0012 airfoil at $(M_\infty = 0.80)$ and $(\alpha = 1.25°)$.

The present isobars for the test case compared with results reported by [7-8] are shown in figure 2. As expected, the two surface shock waves are captured in the present investigation while in the other investigations only the upper shock wave is captured and the lower one is often hardly noticeable [7-8]. In a similar study [17], where adaptive grid is used the lower surface shock wave is also captured.

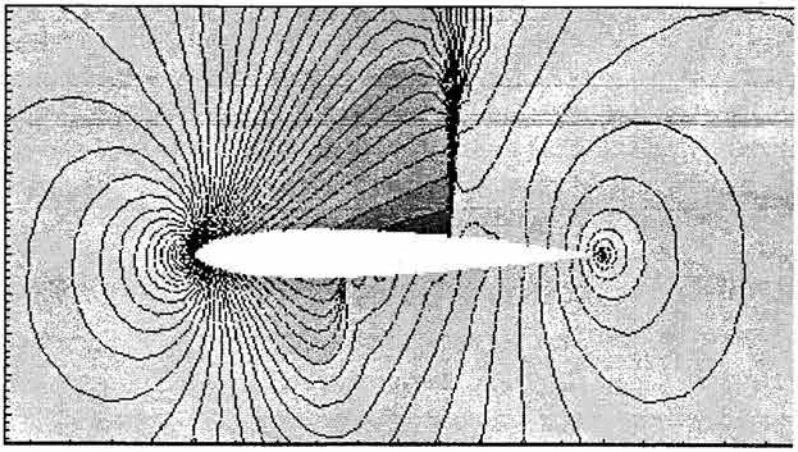

Fig. 2: Isobars (Δp = 0.025) for NACA 0012 transonic flow, $(M_\infty = 0.80)$ and $(\alpha = 1.25°)$

The two shock waves are represented in the corresponding surface-pressure distributions in figure 3. In this figure, the distribution of the coefficient of pressure (C_p) is compared to results from [7]. The computations reveal the sharp shock-capturing ability of the present solver. The shock locations compare favorably with previous solutions. It can be seen that the limiter is very effective in suppressing oscillations and yield a remarkable agreement of pressure distribution with the previous computations [17].

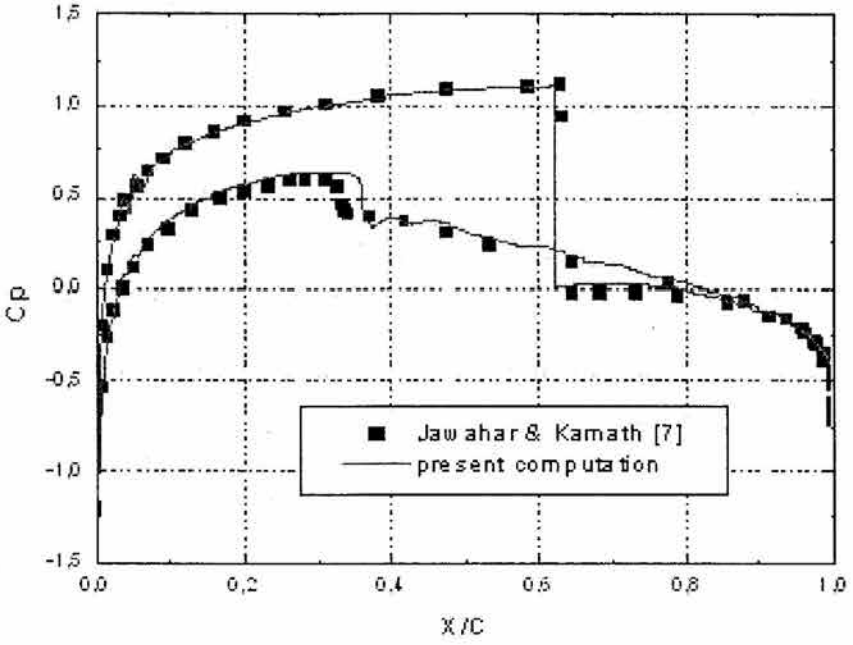

Fig. 3: Surface pressure distribution for NACA 0012 transonic flow, $(M_\infty = 0.80)$ and $(\alpha = 1.25°)$

4. VISCOUS FLOW PAST A TYPICAL AIRFOIL

Viscous flow past a NACA 0012 airfoil is solved and compared with previous computations [7]. The flow parameters used in the simulation are free-stream Mach number $(M_\infty = 0.80)$, angle of attack $(\alpha = 10°)$ and $(Re_\infty = 500)$. This case is characterized by the presence of a large separated region on the upper surface of the airfoil. The objective of this numerical calculation is to demonstrate the ability of the present solver to reproduce accurately the complex flow features using unstructured grids. The computations presented in this study are realized with 16561 points, 32564 elements and 522 points on the airfoil surface. The computational points are clustered near the surface of the airfoil.

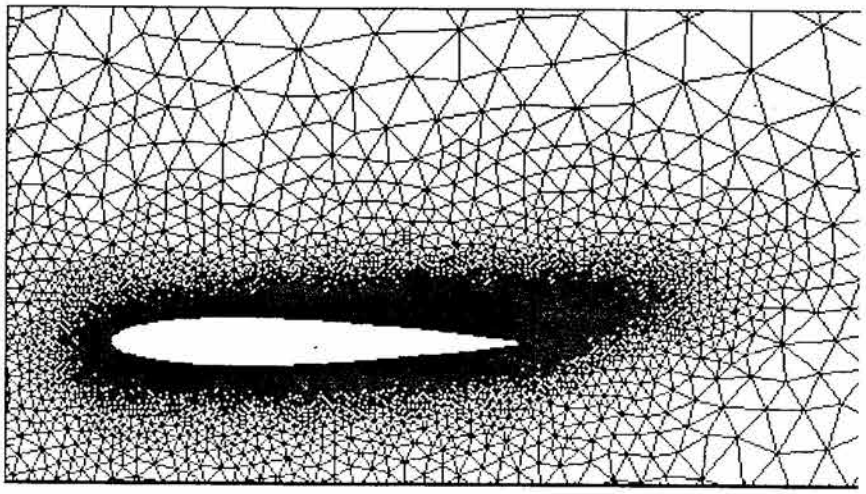

Fig. 4: Close-up of regenerated mesh, Viscous-flow $(M_\infty = 0.80), (\alpha = 10°)$ and $(Re_\infty = 500)$

Figure 4 shows the computational grid obtained after many adaptation steps. It should be pointed out that in order to accurately solve the boundary layer, the size of the cell in a direction normal to the boundary layer should be adequately small.

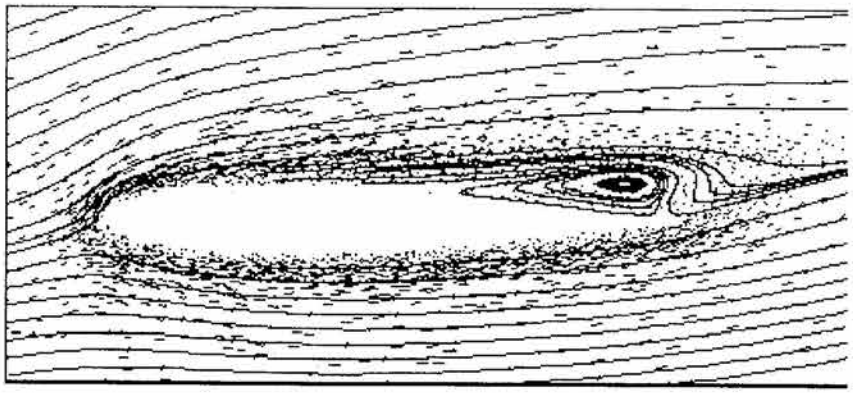

Fig. 5: Laminar viscous flow around NACA0012 airfoil. Streamlines in the separation region $(M_\infty = 0.80)$, $(\alpha = 10°)$ and $(Re_\infty = 500)$

The vortex presented on figure 5 extends over 5% of the chord on the upper surface and compares well with previous computations [7, 15]. The surface-pressure and skin-friction distributions are presented in figures 6 and 7. The overall profiles are similar to those reported in the literature [7].

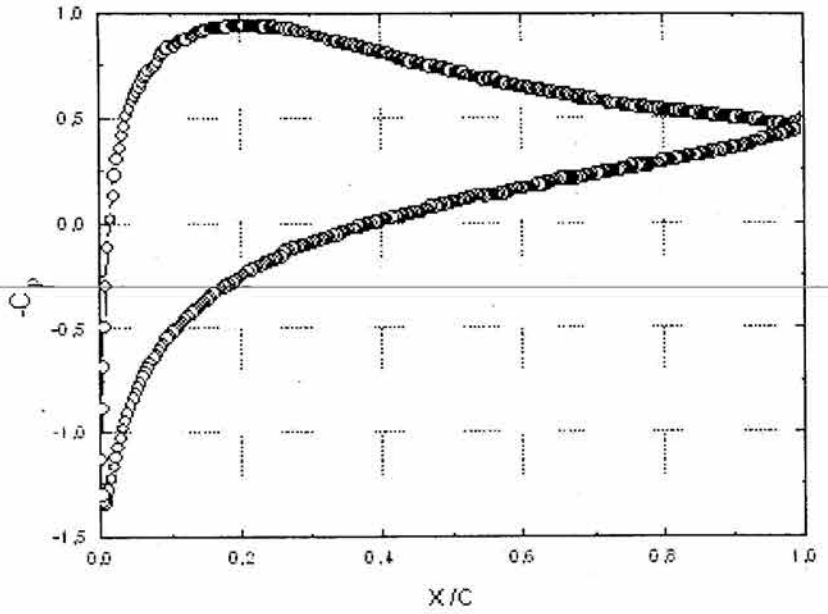

Fig. 6: Pressure distribution, Viscous-flow , $(M_\infty = 0.80), (\alpha = 10°)$ and $(Re_\infty = 500)$

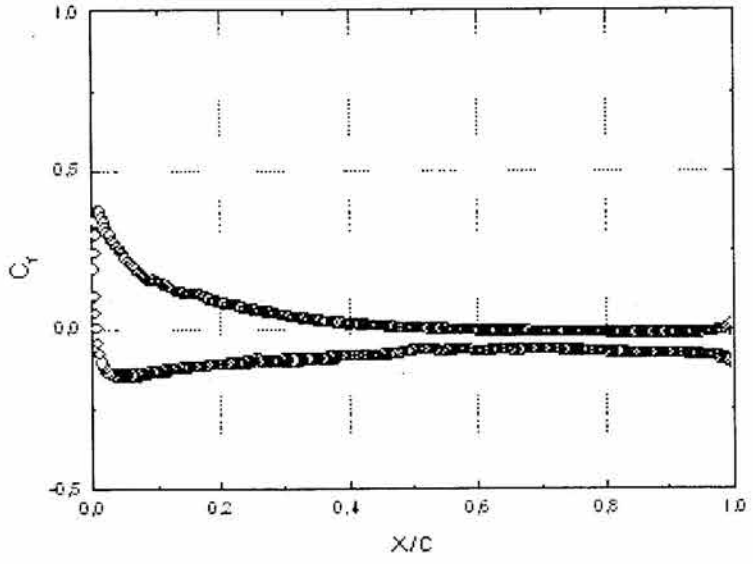

Fig. 7: Skin-friction distribution for a viscous-flow $(M_\infty = 0.80), (\alpha = 10°)$ and $(Re_\infty = 500)$

5. UNSTEADY VISCOUS FLOW PAST A CYLINDER

The vortex shedding behind a circular cylinder is used to validate the present solver. It is well known that in such a flow and for Re > 35, the wake consists of pairs of vortices that shed alternately from the upper and lower part of the rear surface that are called the Kármán vortex streets [18]. Even with fixed and steady boundary conditions, the unsteadiness occurs because of flow instability. The Strouhal number which characterize the dimensionless

cylinder shedding frequency is established around a fixed value equal to *0.2* [16]. The grid used in the present study to compute such a flow (*Re = 150* and *Mach = 0.5*) is composed of 9230 nodes and 18284 triangles as shown on figure 8.

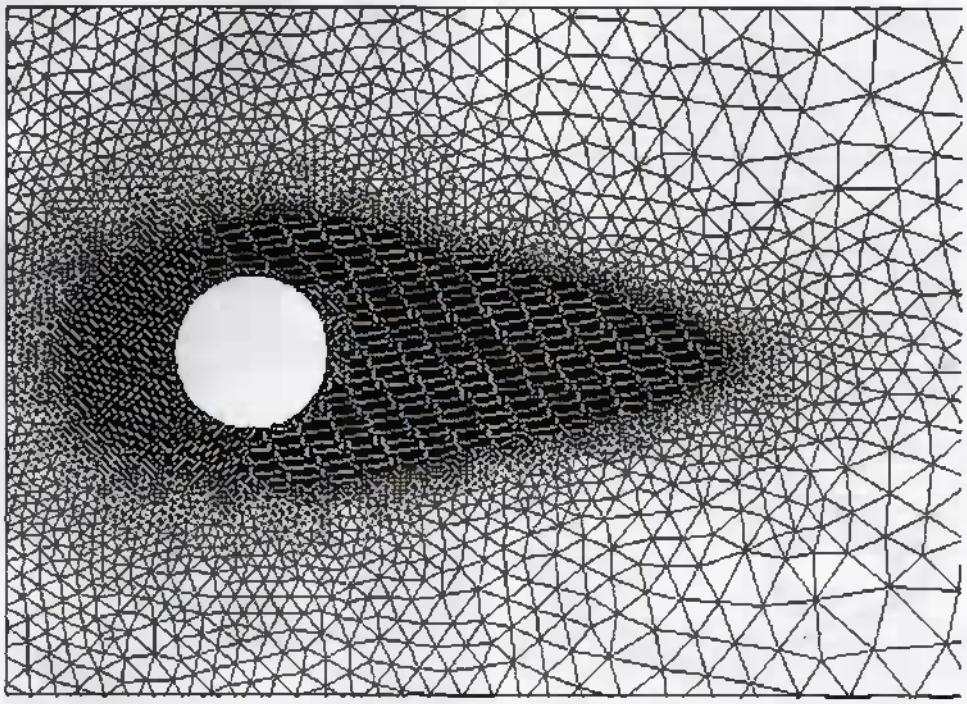

Fig. 8: Close-up of adaptive meshes for a circular cylinder at $(M_\infty = 0.50)$ and $(\mathrm{Re}_\infty = 150)$.

While in the steady situation, the local time step is used, it is necessary to use a global time step when an unsteady calculation is carried out. The global time step is defined as the minimum of the local time step computed for the whole domain. In such situation, the convergence becomes more and more slow. Figure 9 shows the instantaneous pictures of the vortex shedding in form of stream lines and Mach number contours in half period.

6. UNSTEADY VISCOUS FLOW PAST A NACA 0012 AIRFOIL.

As for the circular cylinder, the vortex streets occur in almost any bluff-body flow and especially downstream airfoils. The case selected in this study is the flow around a NACA0012 with the following conditions (*Re = 22000, Mach = 0.1* and *angle of attack = 30°*). We have done more than *50000* iterations to reach the time *t = 62 secs* with an optimized computational grid obtained after many adaptations. The structure of the flow is presented in figure 10 by a selection of instantaneous views in one period, (*f = 0.125 Hz*).

7. CONCLUSION

A high-resolution procedure has been tested for Euler and Navier-Stokes computations on unstructured grids. Numerical computations have confirmed the oscillation-removal capability of the Von Albada limitor. The capability of the adaptive grid technique to produce accurate solution with an optimal distribution of the vertexes is also demonstrated. The modern techniques cited above are applied to predict the details of the challenging transonic compressible inviscid and viscous flows around a NACA 0012 airfoil. After validation with the unsteady flow behind a circular cylinder, the code was successfully applied to the

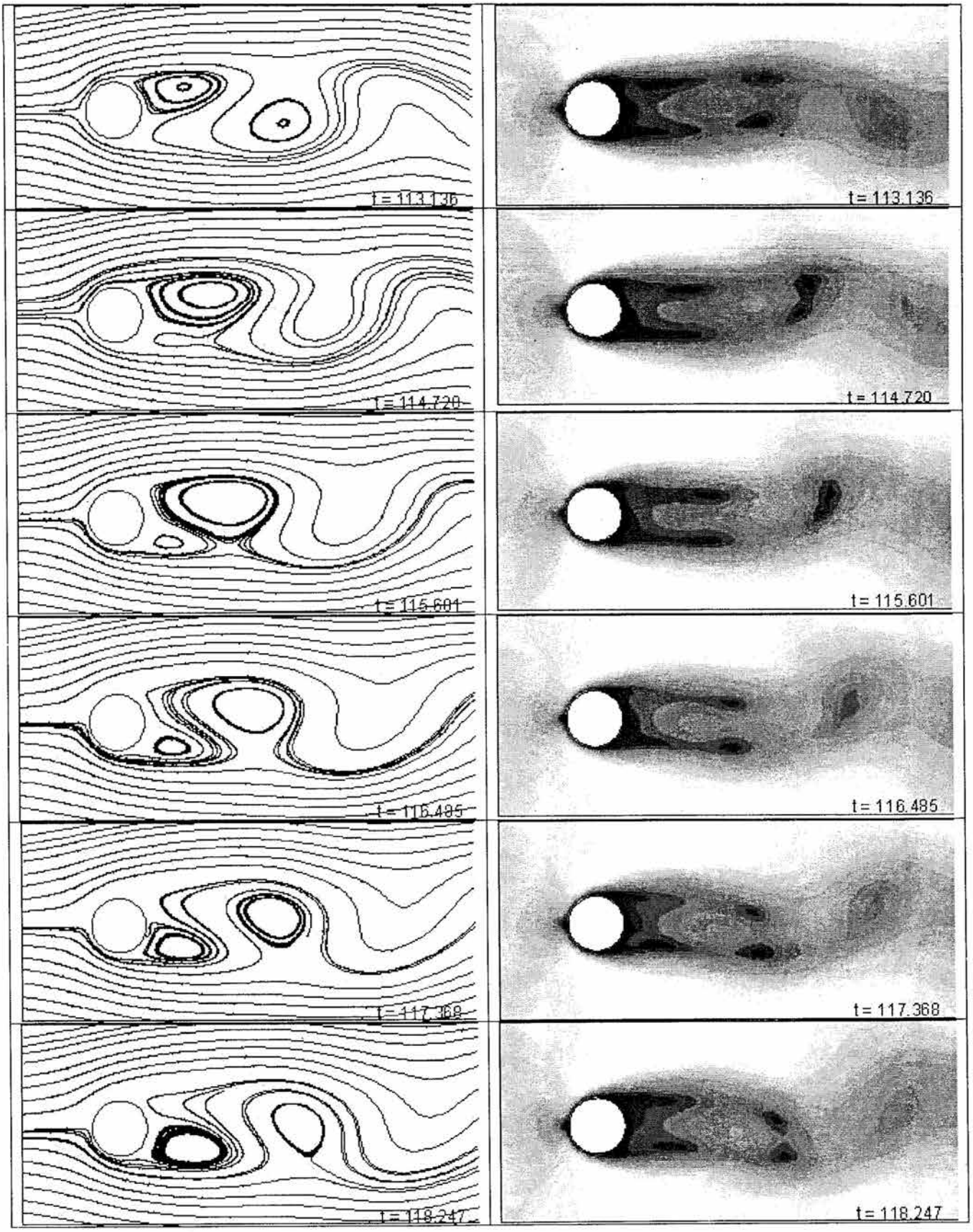

Fig. 9: Instantaneous stream line and Mach number contours behind circular a cylinder $(M_\infty = 0.50)$ and $(\mathrm{Re}_\infty = 150)$ (Times are in seconds).

numerical prediction of an unsteady flow past a NACA 0012 airfoil with excessive relative inclination.

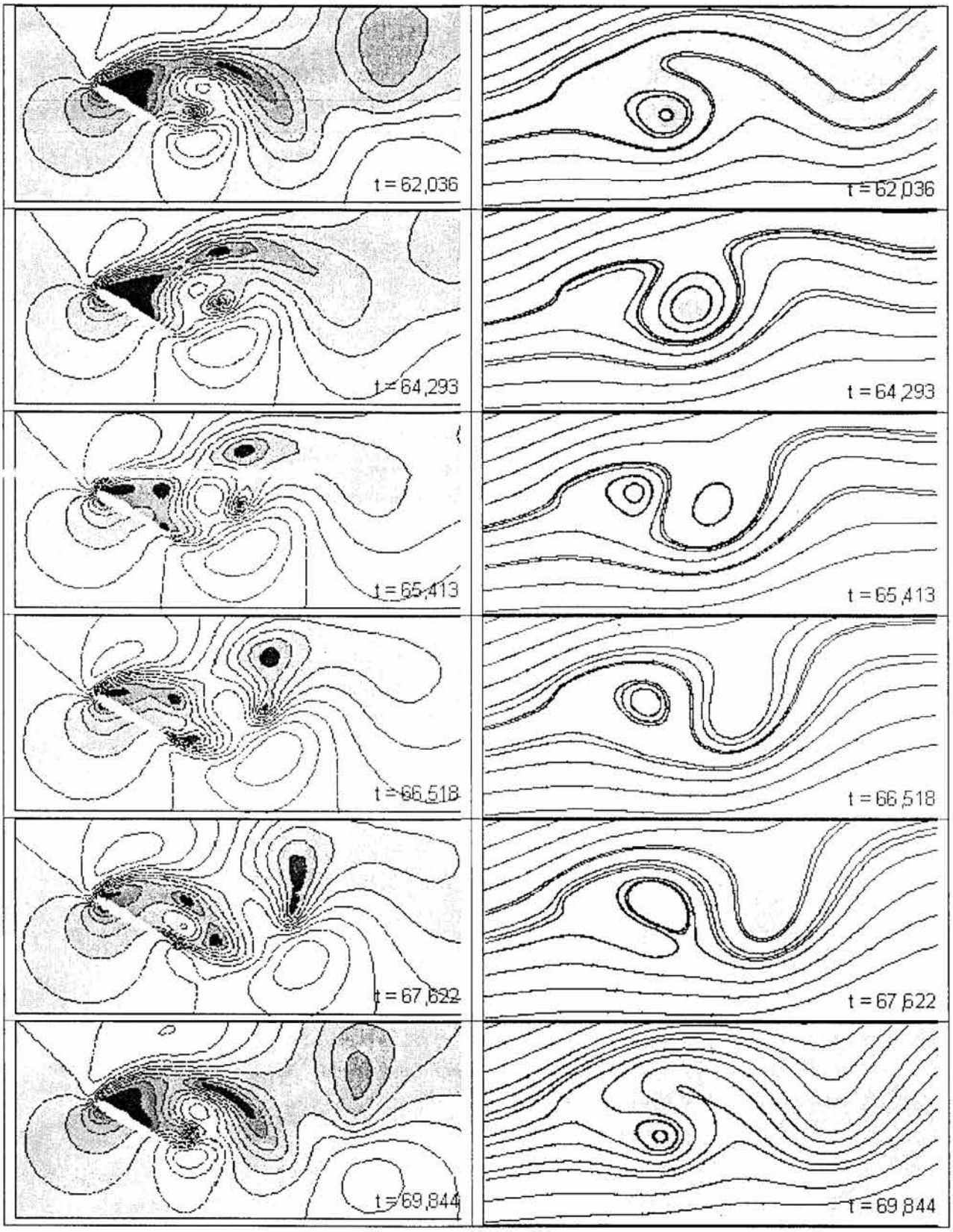

Fig. 10: Instantaneous Mach number contours and stream lines NACA0012, (*Re = 22000, Mach = 0.1* and *angle of attack = 30°*) (Times are in seconds).

Acknowledgements: The authors acknowledge Dr. B. Mohammadi from INRIA, France for providing the NSC2KE solver and Francis X. Giraldo from Naval Research Laboratory, Montrey for providing the Mesh2D grid generation program.

NOMENCLATURE

A	area of the computational cell	Pr	Prandtl number
E	total energy	Re	Reynolds number
F,G	convective flux vectors	St	Strouhal number
F_v,G_v	viscous flux vectors	t	time
H	total enthalpy	U	cell averaged value
M_∞	Mach number	u,v	cartesian velocity components
p	static pressure	x,y	cartesian coordinates
ρ	density	μ	molecular viscosity
$\tau_{xx},\tau_{yy},\tau_{xy}$	viscous stresses	γ	specific heat ratio

REFERENCES

[1] J. T. Bartina, "*Progress in untructured-grid methods development for unsteady aerodynamic applications*", 7th IMACS international conference on computer methods for partial differential equations, Rutgers University, New Jersy USA, June 22-24, 1992.

[2] V. Venkatakrishnan, "*Perspective on unstructured grid flow solvers* ", *AIAA J.* 34(3), (1996)533.

[3] D. J. Mavriplis, "*Unstructured grid techniques* ", Annu. Rev. Fluid. Mech. 29 (1997) 473.

[4] T. J. Barth, "*Aspects of unstructured grids and finite-volume solvers for the Euler and Navier-Stokes equations*", AGARD Rep. 787 (1992).

[5] B. van Leer, "*Towards the ultimate conservative difference scheme V, A second order sequel to Godunov's method*", J. Comput. Phys 32 (1979) 11.

[6] G. D. van Albada, B. van Leer, and W. W. Roberts, "*A comparative study of computational methods in cosmic gas dynamics*", Astron. Astrophys. 108 (1982) 76.

[7] P. Jawahar and H. Kamath, "*A High-Resolution Procedure for Euler and Navier-Stokes Computations on Unstructured Grids*", Journal of Computational Physics 164 (2000) 165-203.

[8] I. Wenneker, G. Segal and P. Wesseling, "*Conservation properties of a new unstructured staggered scheme, Accepted for publication in Computers & Fluids.*", http://ta.twi.tudelft.nl/unstructured_fvm/compfluids.pdf.

[9] J. R. Amaladas and H. Kamath, "*Accuracy assessment of upwind algorithms for steady-state equations*", Comput. Fluids 27 (8) (1998) 941.

[10] B. Mohammadi, "*Fluid Dynamics Computation with NSC2KE An User-Guide, Release 1.0*", INRIA, N° RT-0164, Mai 1994.

[11] P. L. Roe; "*Approximate Riemann Solver, Parameters Vectors and Differences Schemes*", J.C.P. Vol. 43, 1981.

[12] H. Yoshihara and P. Sacher,"*Test cases for inviscid flow field method*", AGARDograph N°.211, AGARD, Neuilly-sur-Seine, France, 1985.A.

[13] T. H. Pulliam and J. T. Barton, "*Euler computations of AGARD working group 07, Airfoil test cases*", AIAA Pap. *85-00187* (1985).

[14] Francis X. Giraldo 9/96, "*Meh2D*", Naval Research Laboratory, Montrey, CA 93943
[15] A. Haselbacher, J. J. McGuirk, and G. J. Page, "*Finite volume discretisation aspects for viscous flows on mixed unstructured grids* ", AIAA J. 37(2), (1999) 177.
[16] O. Inoue, T. Yamasaki, and T. Bisaka, "*Numerical simulation of forced Wakes around a Cylinder* ". Int. J. Heat and Fluid Flow18 (1995) 327-332..
[17] R. D. Rausch, J. T. Batina and H. T. Y. Yang, "*Spatial Adaptation Procedures on Unstructured Meshes for Accurate Unsteady Aerodynamic Flow Computation*", AIAA paper N°. 91-1106, 1991.
[18] Frank M. White, "*Viscous Fluid Flow*", McGraw-Hill, Inc, 2nd ed.